The detection of ionospheric trough with GNSS measurements.

Rafał Sieradzki, Jacek Paziewski, *University of Warmia and Mazury in Olsztyn, Poland*

rafal.sieradzki@uwm.edu.pl, jacek.paziewski@uwm.edu.pl

INTRODUCTION

The main ionospheric trough represents a large scale depletion of plasma density elongated in longitude, which is typically observed at the boundary between high- and mid-latitude ionosphere. The trough is characterized by a steep density gradient in a poleward direction and gradual on the equatorward site. According to the recent studies, it begins in the late afternoon, moves equatorward during the night hours and rapidly retreats to higher latitudes at a dawn. Due to the dynamic of auroral oval, this ionospheric feature exhibits a temporal variability and shifts equatorward during the geomagnetic activity.

METHODOLOGY OF GNSS-BASED DETECTION OF IONOSPHERIC TROUGH

The recent investigations aimed at characterization of high latitude ionosphere demonstrated that appropriate processing of GNSS data can provide the very detailed view of polar and auroral disturbances. Furthermore, the conducted analysis involved also mid-latitudes and revealed that the adopted indicator - relative STEC values - is sensitive to ionospheric trough as well (Sieradzki and Paziewski, 2019). The example of such signature in the nightside sector of ionosphere at ~45° of geomagnetic latitude demonstrates Fig. 1.

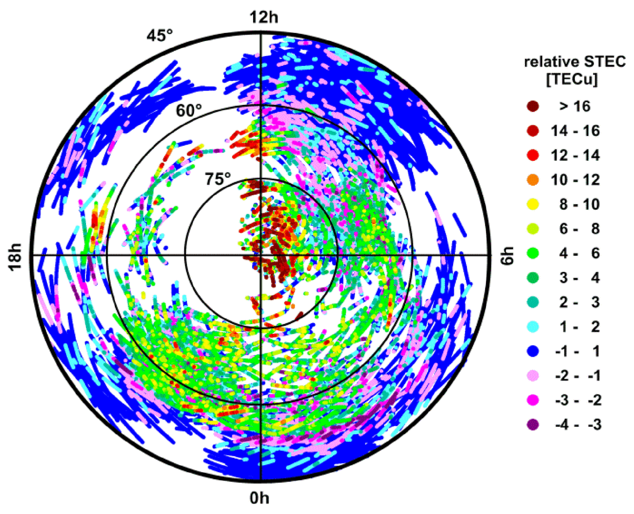

Fig.1 The map of relative STEC values (8:00–10:00 UT, March 7, 2012) as a function of geomagnetic latitude and MLT (Sieradzki and Paziewski, 2019).

Thus, the next step of research was the verification if time series of single-arc observables can be used for visualization of ionospheric trough. The analysis of network-derived relative STEC values confirmed the occurence of this phenomenon but also indicated that their extraction may be problematic. In contrast to high-latitude irregularities, ionospheric trough is spatially extended and the approach proposed for patch detection could be effective only in limited number of cases (such in Fig. 1). On the other hand, the positive consequence of this spatial coverage is a feasibility of simple conversion from slant to vertical TEC what allows normalization the data in particular arc as soon as the one sample is aligned to a selected reference level.

Finally, the algorithm consists of a few general steps. The starting point of algorithm is cleaning of phase data performed as follows. At first, the large cycle-slips are detected using temporal differences of L_4 with the threshold limit set to 5 TECu/min. Then, each clean part of an arc longer than 15 minutes is levelled to code data according to equation.

$$\tilde{\mathrm{L}}_{4(\mathrm{k})} = \mathrm{L}_{4(\mathrm{k})} - \mathrm{median}(\mathrm{L}_{4(\mathrm{k})} + \mathrm{P}_{4(\mathrm{k})})_{\mathrm{arc}}$$

In the case of the shorter periods, which are characterized by cycle-slips, they are replaced with a five-epoch moving average of $-P_{4(k)}$. This process slightly smooths the pattern of structures in the time domain, but we think it does not distort the trough signature significantly.

The next step is levelling of slant TEC time series using global ionosphere maps. For this purpose we select an epoch and compute slant TEC from the global map using cos(z') function (z' – zenith angle at the ionospheric point). Then, we shift the entire time series of geometry-free data to the reference values from map. At the end all data in arc are converted to VTEC using the same cos(z') function.

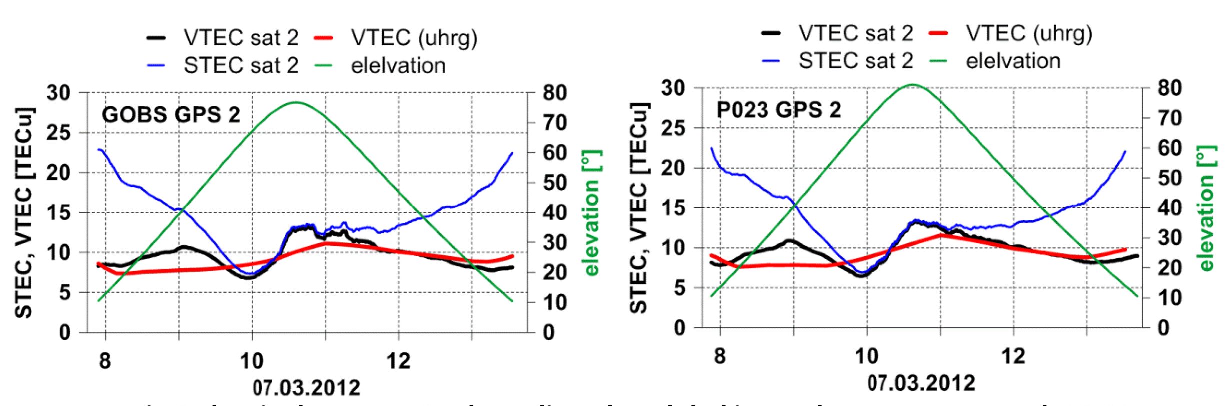

Fig.2 The single-arc VTEC values aligned to global ionosphere maps at epoch 12:00

Fig. 2 demonstrates the processing of geometry-free data for two example arcs with an elevation mask set to 10°. The clean levelled STEC data for particular satellite are given in blue, whereas converted VTEC data are marked with black. The latter values are aligned to VTEC from hourly UPC map at 12:00 UTC. The reference epoch seems to be the key for appropriate combining the data from different stations. It should fulfil two requirements: a possibly high elevation and quiet ionosphere. In our case the measurements with the highest elevations were affected by trough signature and thus, the selected epoch is a good compromise.

A case of geomagnetic storm – March 7, 2012

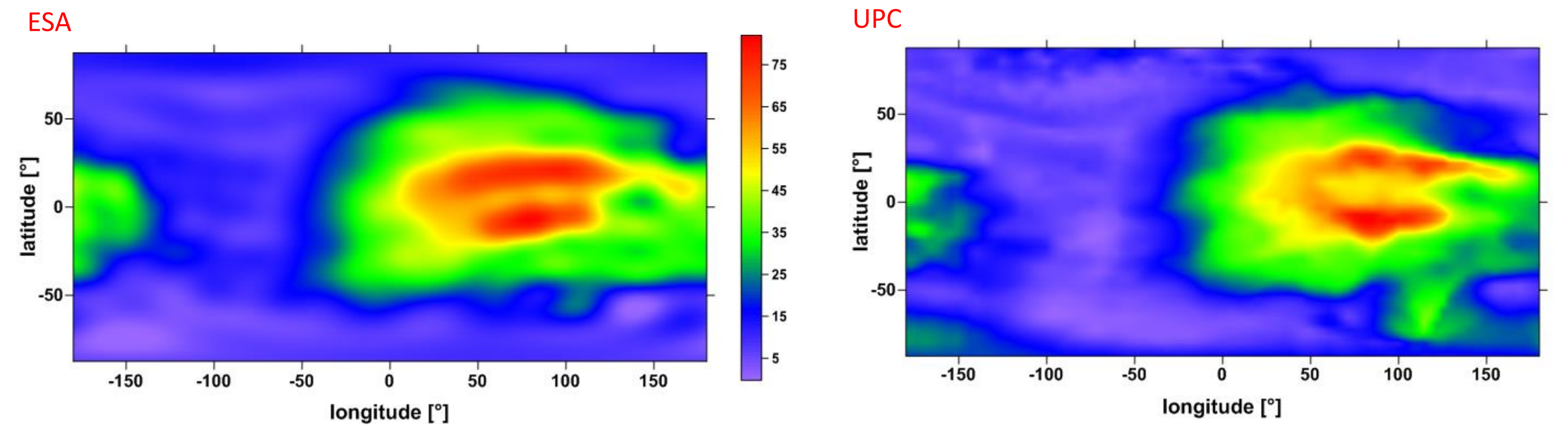

Fig.3 Hourly maps of ionosphere provided by ESA (left panel) and UPC (right panel), March 7, 2012, 10:00 UTC.

The first case concerns the situation given in Fig. 1, i.e. the ionospheric trough near the peak of the geomagnetic storm on March 7, 2012. As it was confirmed in our previous investigations, the auroral oval was then extremely expanded and consequently the ionospheric trough was also moved equatorward. The preliminary step of analysis involved the verification what conditions demonstrate the global ionospheric maps (Fig. 3). For this purpose we used the products provided by ESA and UPC (Feltens 1998 and Hernández-Pajares et al. 1999). As one can observe VTEC differs significantly in both these cases. There is no doubt that the map generated by ESA is smoother what is probably related to spherical harmonic expansion applied for VTEC representation. For presentation single-arc VTEC (referenced to UPC map at epoch 12:00), we used ~16 stations from Plate Boundary Observatory mission which is acknowledged (Fig. 4). Such linear sub-network of permanent stations allows clear visualization of ionospheric trough for different longitudes.

Fig. 5 presents the comparison of trough signature derived from global VTEC maps and single-arc data. In the second case we generated the maps using measurements from 2 GPS satellites (PRN 2 and 4). According to the results in the top panel, the signatures of trough can be noticed on both ionospheric maps. Probably due to the applied algorithm of interpolation (kriging), the product of UPC provide more real shape of ionosphere. Nevertheless, only the maps derived from single-arc data depict the true ionospheric conditions. In specific they demonstrate the sharp edges of ionospheric trough and its compression in the latitude direction.

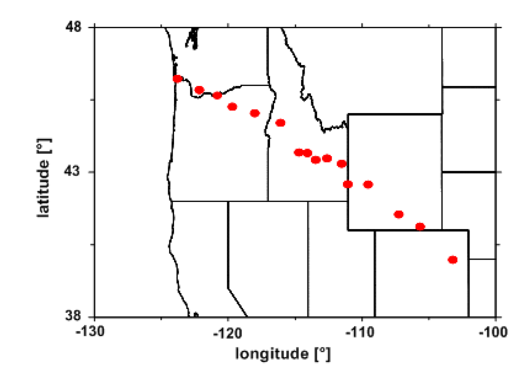

Fig. 4 Distribution of the permanent stations used in experiment.

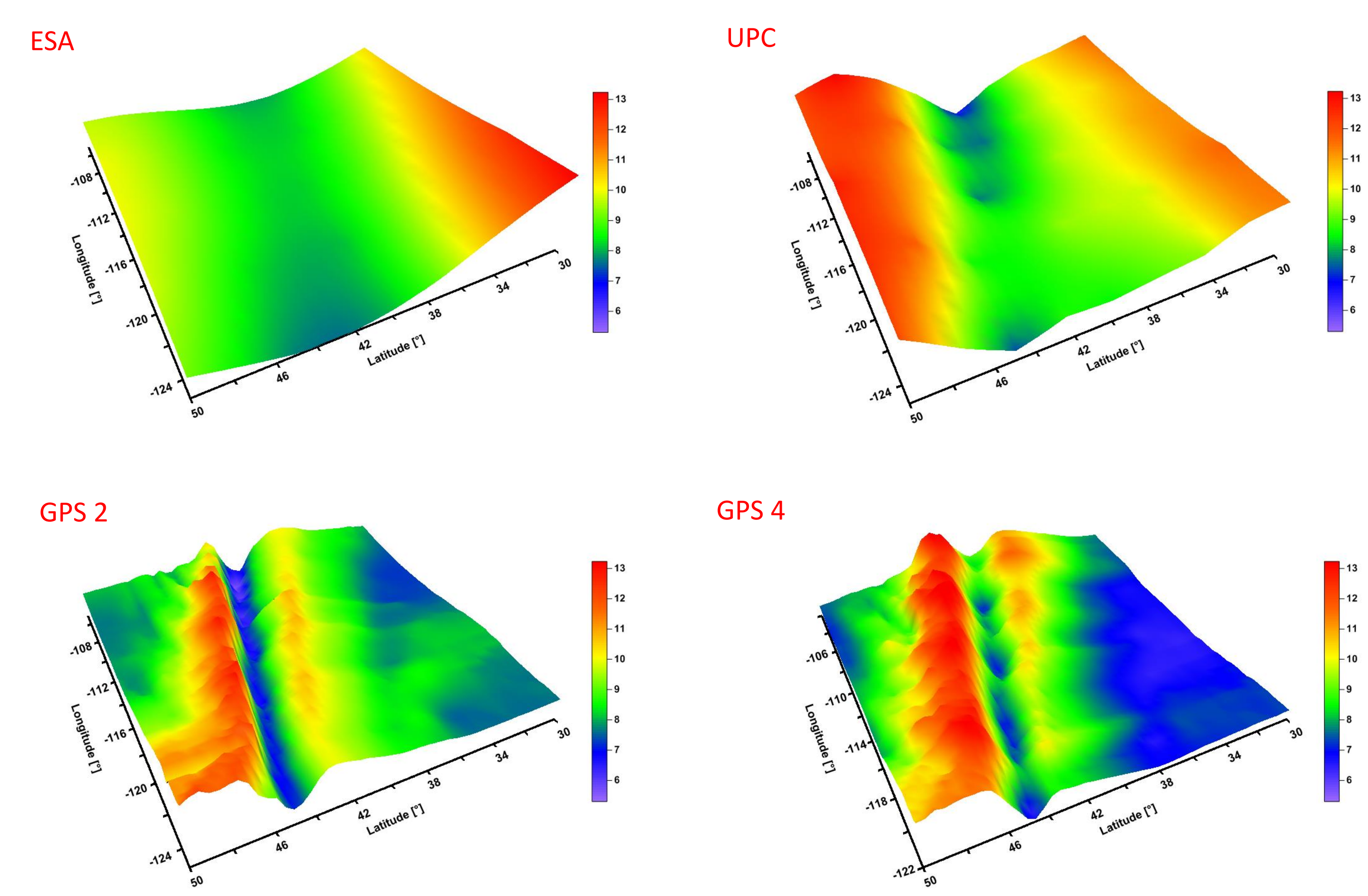

Fig. 5 Comparison of the ionospheric VTEC maps (ESA, UPC) with the VTEC derived from single satellites (GPS 2 and GPS 4).

A case of depleted ionosphere – March 8, 2012

The second case depicts the conditions just after a long period of northwardly oriented IMF, which was combined with negative recovery phase after the storm which occured on March 7, 2012. The consequence of the reorientation was strong increase of plasma in the auroral oval, related probably to an oval-aligned arc. On the other the negative phase of the storm implicated the global depletion of the ionosphere. Both these factors lead to a sharp gradient observed at the equatorward boundary auroral oval – ionospheric trough. The position of this boundary was located at higher latitudes and thus, we used GNSS data from PBO stations located mostly in Alaska (Fig. 6). Looking at the comparison of the results from different sources (Fig. 7) we can see that UPC map captured the strong gradient at the equatorward boundary of oval. On the other hand, the applied interpolation caused its smoothing in latitude direction. The single-arc results provide the real scale of difference in amount of plasma on both sides of boundary, which exceeds 10 TECu. Furthermore, the results depict that there was extensively long depletion without an increase of TEC up to 45° latitude. Comparing the results for both satellites one can observe a shift in boundary position, which is related to slightly different epochs of trough signature.

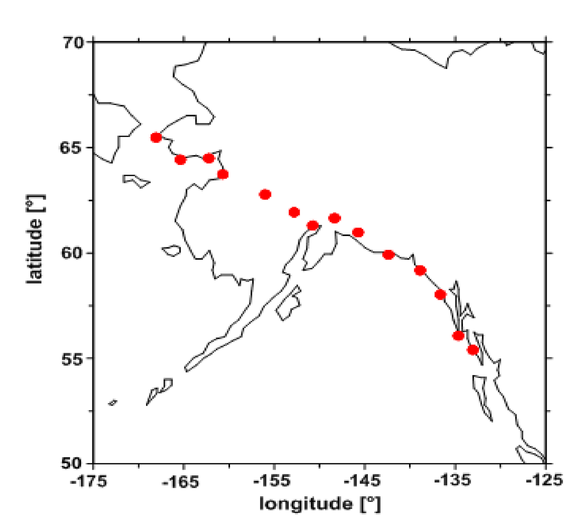

Fig. 6 Distribution of the permanent stations used in experiment.

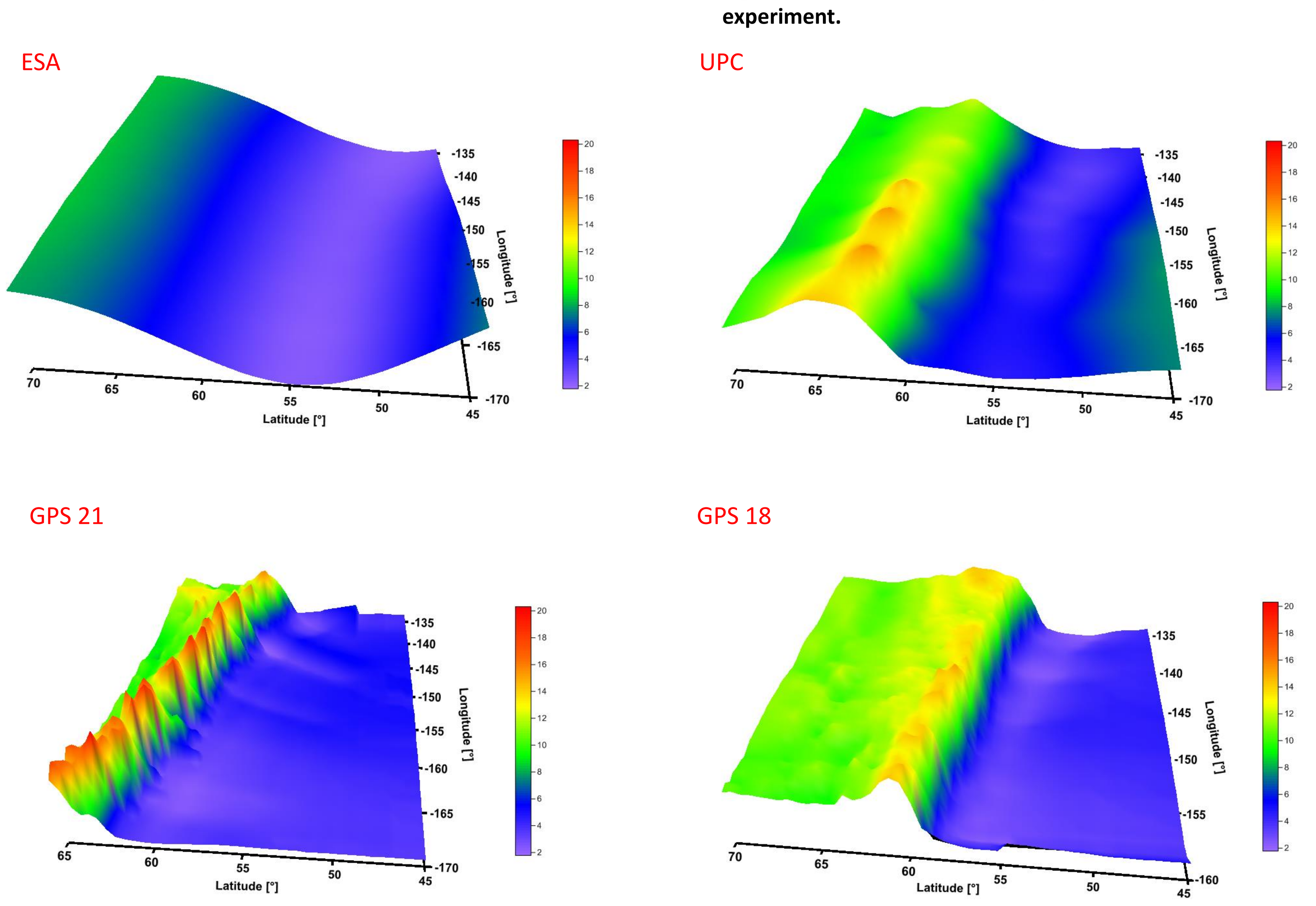

Fig. 7 Comparison of ionospheric VTEC maps (ESA, UPC) with VTEC derived from single satellites (GPS 21 and GPS 18).

CONCLUSIONS

- The particular ionospheric maps are based on different algorithms and thus their efficiency in depicting of ionospheric trough varies significantly. This may be also related to different datasets used for maps preparation.
- As demonstrated, the time series of geometry-free observables can be used for detection of ionospheric trough at the northern hemisphere. The variations of slant TEC, derived directly from dual-frequency data, can be aligned to a ionospheric map and consequently converted to VTEC values. The application of the proposed algorithm to linear network of GNSS stations provides the detailed spatial view on ionospheric conditions.
- The results for different satellites are basically consistent. The discrepancies seem to be related to different epoch of trough signatures. In the analyzed cases the trough was observed simultaneously only by a few GPS satellites. On the other hand, one can expect that multi-GNSS receivers should improve applicability of the proposed algorithm.
- The comparison of different results indicates that the main advantage of the detection based on single arc data is providing sharp ionospheric signatures, which is not possible for VTEC maps. This is especially true at the edges of the trough. As a consequence we can detect a compressed depletion for the main phase of geomagnetic storm.
- In both analyzed cases VTEC depletion exceeded 10 TECu and was extremely rapid (about one degree in latitudinal direction).
- The promising results suggest that the proposed algorithm can be applied for more detailed statistical studies of ionospheric trough

REFERENCES

- Feltens, J., 1998, Chapman Profile Approach for 3-D Global TEC Representation, IGS Presentation, in proceedings of the 1998 IGS Analysis Centers Workshop, ESOC, Darmstadt, Germany, February 9-11, 1998 pp. 285-297.
- Hernández-Pajares M., Juan J.M. and Sanz J., 1999, New approaches in global ionospheric determination using ground GPS data, Journal of Atmospheric and Solar Terrestrial Physics, vol. 61, pp. 1237-1247.
- Sieradzki, R., Paziewski, J., 2019, GNSS-based analysis of high latitude ionospheric response on a sequence of geomagnetic storms performed with ROTI and a new relative STEC indicator. J. Space Weather Space Clim. 9, A5.

ACKNOWLEDGMENTS

This work was supported by the National Science Centre, Poland: project No. 2016/23/D/ST10/01546. The authors are grateful for GNSS data provided by IGS and UNAVCO.